J. Am. Chem. Soc. 1983, 105, 4571–4575

disorder could be detected. The sulfur atom is highly anisotropic. The final R_{obsd} factor is 8.3%.

TOT·(*R*,*R*)-(+)-9. Crystal structure determination had the same characteristics as that of TOT·(*S*,*S*)-(−)-**10**; the final R_{obsd} factor is 6.4%.

Acknowledgment. We are grateful to Professor V. Schurig and W. Bürkle for the analyses of guests **10–13** and for fruitful discussions. We thank Professor G. M. Whitesides for sending us a sample of chiral Eu(III) reagent. TOT was synthesized by A. Jacob; we thank her and F. Villain for technical assistance. This research received support from the CNRS (as part of ATP No. 2662 on "Chiral Structures" with NCRD, Jerusalem) and the Israel Academy of Sciences.

Supplementary Material Available: Atomic coordinates and thermal parameters in cage-type clathrates with 2-bromobutane, enantiomerically pure 2,3-dimethyloxirane, enantiomerically pure 2,3-dimethylthiirane, and 66% enantiomerically enriched 2,3-dimethylthiirane as guests, and observed and calculated structure factors for (−)TOT·(*R*,*R*)-(+)-2,3-dimethyloxirane (31 pages). Ordering information is given on any current masthead page.

Electronic Absorption and Emission Spectra of Binuclear Platinum(II) Complexes. Characterization of the Lowest Singlet and Triplet Excited States of $Pt_2(H_2P_2O_5)_4{}^{4-}$

Steven F. Rice and Harry B. Gray*

Contribution No. 6712 from the Arthur Amos Noyes Laboratory, California Institute of Technology, Pasadena, California 91125. *Received August 30, 1982*

Abstract: The low-temperature electronic absorption and emission spectra of single crystals containing a binuclear platinum anion, $Pt_2(H_2P_2O_5)_4{}^{4-}$, have been measured and analyzed. Absorption systems in the 450- and 360-nm regions are attributable to transitions to $d\sigma^*p\sigma$ excited states ($^3A_{2u}$ and $^1A_{2u}$, respectively). The Pt–Pt stretching frequency in the $^3A_{2u}$ state (155 cm^{-1}) is much larger than that (110 cm^{-1}) in the ground state (the $^3A_{2u}$ absorption as well as the fluorescence ($^1A_{2u} \rightarrow {}^1A_{1g}$) and phosphorescence ($^3A_{2u} \rightarrow {}^1A_{1g}$) spectra exhibit Pt–Pt stretching progressions), which accords with the $d\sigma^*p\sigma$ description of the excited state. The Pt–Pt bond is calculated to contract by 0.21 Å in the $^3A_{2u}$ state (relative to the ground-state value of 2.92 Å). Measurements of the phosphorescence spectrum of $Ba_2Pt_2(H_2P_2O_5)_4$ at low temperatures (8–4.2 K) confirm that there are two emitting levels split by 40.9 cm^{-1} (origins at 476.55 and 477.48 nm are assigned to the E_u and A_{1u} spin–orbit components of $^3A_{2u}$).

Our previous studies of the electronic spectroscopy and photochemistry of binuclear d^8·d^8 complexes have centered mainly on rhodium(I) systems, whose lowest excited state ($^3A_{2u}$; $(d\sigma)^2(d\sigma^*)^1(p\sigma)^1$) possesses a relatively strong Rh–Rh bond.[1-3] If our description of the d^8·d^8 interaction is correct, then it should be possible to manipulate the photophysical and photochemical properties of these systems by appropriate variations in the metal–metal interactions. In this context we have found that the intensely luminescent[4] platinum(II) complex,[5] $Pt_2(H_2P_2O_5)_4{}^{4-}$, is a most attractive system for study.[6] The excited-state lifetime of the potassium salt of this complex, $K_4Pt_2(H_2P_2O_5)_4 \cdot 2H_2O$ (Pt–Pt = 2.922 Å),[5] has been measured over a wide temperature range by Fordyce, Brummer, and Crosby.[7] From the latter study the zero-field splitting of $^3A_{2u}$ was estimated to be 49 cm^{-1}.

We now have developed a detailed electronic structural picture of binuclear d^8·d^8 systems through high resolution absorption and emission spectroscopic studies of single crystals of $Ba_2Pt_2(H_2P_2O_5)_4$. We have observed two emitting levels in the $^3A_{2u}$ region, thereby verifying the most important aspect of the Fordyce–Brummer–Crosby analysis.[7] Furthermore, we have elucidated fully the nature of the Pt–Pt bonding and other key aspects of structure in the lowest excited states of $Pt_2(H_2P_2O_5)_4{}^{4-}$.

Experimental Section

Instrumentation. Absorption spectra were measured on a Cary 17 absorption spectrometer equipped with a Hamamatsu R955 photomultiplier tube. Emission spectra were measured as follows: Light from a Hanovia 200 W Hg/Xe arc lamp was wavelength selected with a Spex Minimate monochromator and modulated at 108 Hz with a PAR Model 125A light chopper before excitation of the sample; the emitted light was dispersed with a Spex 1780 0.5-m monochromator and detected with a Hamamatsu R955 PMT; the signal was amplified with a PAR Model 186A lock-in amplifier equipped with a PAR 181 current sensitive preamplifier and displayed on a chart recorder. An Andonian O-24 variable-temperature liquid-helium optical dewar was used to obtain spectra at low temperatures. The sample temperature was measured with a calibrated 500 Ω carbon–glass resistor imbedded in a brass block near the sample.

Sample Preparation. $K_4Pt_2(H_2P_2O_5)_4 \cdot 2H_2O$. A crude green sample of $K_4Pt_2(H_2P_2O_5)_4 \cdot 2H_2O$ was prepared by the method of Sadler.[5] It was precipitated from water by the addition of methanol to yield a yellow microcrystalline material. Pure yellow single crystals of $K_4Pt_2(H_2P_2O_5)_4 \cdot 2H_2O$ were grown as follows: Freshly precipitated $K_4Pt_2(H_2P_2O_5)_4$ (1.5 g) was dried on a vacuum line and then dissolved in 40 mL of degassed H_2O added to the powder by bulb-to-bulb distillation. The water was then slowly distilled away from the compound over several days by connecting the sample flask to a flask immersed in salted ice at −2 °C. In this way crystals could be grown in the absence of oxygen.

This method would on occasion yield very large (5 × 5 × 1 mm) bright yellow crystals with optical properties consistent with a tetragonal space group. X-ray photographs were taken of several of these samples. They displayed the same space group and unit cell dimensions as those obtained by Sadler. The crystals were typically square slabs exhibiting the 001 face with 110, $\bar{1}10$, $1\bar{1}0$, and $\bar{1}\bar{1}0$ faces as edges. Occasionally, 2 × 1 × 1 mm rectangular blocks were obtained with 110 and 001 faces as the larger surfaces.

$Ba_2Pt_2(H_2P_2O_5)_4$. Three tenths of a gram of the potassium salt was dissolved in 10 mL of H_2O. An aqueous solution (10 mL) containing 1.0 g of $Ba(ClO_4)_2$ was added to this solution. Large yellow-green plates formed after several hours. These crystals exhibited a two-symmetry-

---

(1) Rice, S. F.; Gray, H. B. *J. Am. Chem. Soc.* **1981**, *103*, 1593–1595.

(2) Mann, K. R.; Thich, J. A.; Bell, R. A.; Coyle, C. L.; Gray, H. B. *Inorg. Chem.* **1980**, *19*, 2462–2468.

(3) Mann, K. R.; Gray, H. B. *Adv. Chem. Ser.* **1979**, *No. 173*, 225–235.

(4) Sperline, R. P.; Dickson, M. K.; Roundhill, D. M. *J. Chem. Soc., Chem. Commun.* **1977**, 62–63.

(5) Filimena Dos Remedios Pinto, M. A.; Sadler, P. J.; Neidle, S.; Sanderson, M. R.; Subbiah, A. *J. Chem. Soc., Chem. Commun.* **1980**, 13–15.

(6) Che, C.-M.; Butler, L. G.; Gray, H. B. *J. Am. Chem. Soc.* **1981**, *103*, 7796–7797.

(7) Fordyce, W. A.; Brummer, J. G.; Crosby, G. A. *J. Am. Chem. Soc.* **1981**, *103*, 7061–7064.

0002-7863/83/1505-4571$01.50/0

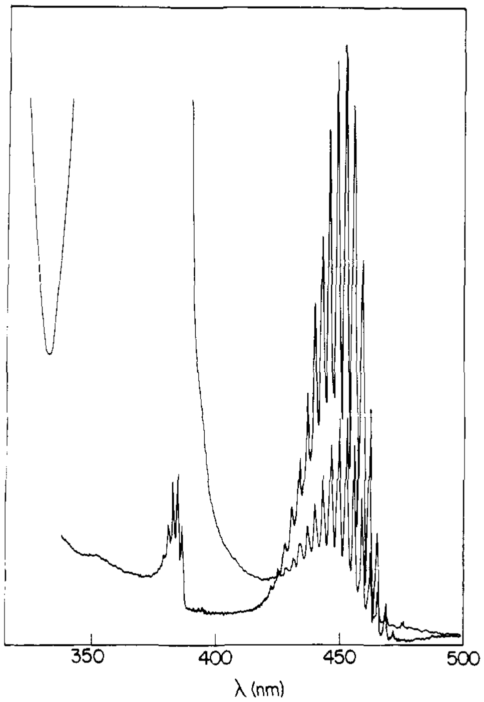

Figure 1. Absorption spectrum along two extinction directions of the same face of a single crystal of $Ba_2Pt_2(H_2P_2O_5)_4$ at 5 K. The orientation of the metal–metal direction is not known in this salt.

plane optical figure on the large face. The extinction directions on this face were both yellow, one being more intense than the other.

Results and Discussion

The room-temperature absorption spectrum of $Pt_2(H_2P_2O_5)_4{}^{4-}$ exhibits an intense band at 360 nm and a weak system at 450 nm that are assigned as transitions to the $d\sigma^*p\sigma$ singlet and triplet excited states (${}^1A_{1g} \rightarrow {}^3A_{2u}$ and ${}^1A_{1g} \rightarrow {}^1A_{2u}$). The absorption spectrum of a thin single crystal of $Ba_2Pt_2(H_2P_2O_5)_4$ at 5 K is shown in Figure 1 for two polarizations. A progression in a low frequency is observed with the maximum of the band occurring about 7 quanta from the origin. The origin is located at 475.9 nm with a $0 \rightarrow 1$ vibrational spacing of 155 cm^{-1}. There is also a very low energy vibration (40 cm^{-1}) built on the origin. The 155-cm^{-1} progression is assigned to the Pt–Pt stretch in the ${}^3A_{2u}$ excited state and the 40-cm^{-1} mode is probably a ligand deformation.[8] Table I lists the positions of all the lines.

A room-temperature polarized spectrum of $K_4Pt_2(H_2P_2O_5)_4 \cdot 2H_2O$ is displayed in Figure 2. The strong x,y polarization of the 450-nm band supports the ${}^1A_{1g} \rightarrow {}^3A_{2u}$ assignment.[9] The intense band in z polarization (360 nm) is ${}^1A_{1g} \rightarrow {}^1A_{2u}$. Unlike the potassium salt, the barium salt has a significant contribution to the ${}^1A_{1g} \rightarrow {}^3A_{2u}$ absorption in both extinction directions. The orientation of the binuclear anion is not known in this salt and it is possible that one of the two directions presented by the crystal could be molecular x,y polarized but the other not purely z polarized. The ${}^1A_{1g} \rightarrow {}^3A_{2u}$ intensity along both these extinction directions could still be entirely x,y as in the case of $K_4Pt_2(H_2P_2O_5)_4 \cdot 2H_2O$.

One more feature in the absorption spectrum of $Pt_2(H_2P_2O_5)_4{}^{4-}$ should be noted. The spectra of both the barium and potassium salts exhibit a structured band at about 400 nm. The band is essentially the same in both salts, having a ~120-cm^{-1} progression that is assumed to be the Pt–Pt stretch, and its intensity profile indicates that the Pt–Pt distortion is relatively small (~0.1 Å).

Table I. Positions and Spacings between the Lines in the ${}^1A_{1g} \rightarrow {}^3A_{2u}$ Absorption Spectrum of $Ba_2Pt_2(H_2P_2O_5)_4$

V^a	E_v, cm^{-1}	Δ^b	$E_v - E_{v-1}$
0	21008		
	21053	40	
1	21163		155
	21199	36	
2	21317		154
	21346	29	
3	21473		156
	21500	27	
4	21626		153
	21651	25	
5	21778		152
	21805	27	
6	21927		149
7	22081		154
8	22234		153
9	22389		155
10	22548		159
11	22706		158
12	22865		159
13	23023		158
14	23175		152
15	23324		149
16	23487		163
17	23631		144
18	23793		162
19	23952		159

[a] The assigned a_{1g}(Pt–Pt) vibrational quantum number.
[b] Spacings between the principal peaks and the secondary (ligand deformation) peaks.

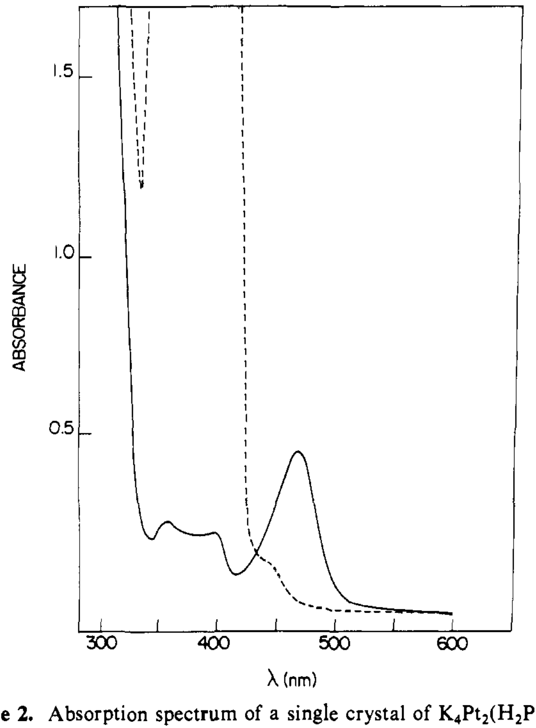

Figure 2. Absorption spectrum of a single crystal of $K_4Pt_2(H_2P_2O_5)_4 \cdot 2H_2O$ at 300 K. Solid line: electric dipole perpendicular to the crystallographic c axis. Dashed line: parallel to the c axis and the Pt–Pt axis.

The intensity of the 400-nm band was not reproducible. Ordinarily, this behavior would be indicative of an impurity absorption. However, the excitation spectrum of the ${}^3A_{2u}$ emission shows the presence of this state, including the fine structure, indicating that the electronic transition in question leads to luminescence from ${}^3A_{2u}$. Provided that energy transfer within the crystal is slower than the decay, the excitation spectrum is strong evidence that this feature corresponds to an authentic state of $Pt_2(H_2P_2O_5)_4{}^{4-}$ and not to an impurity. Recall that the ion orientations, and therefore the transition dipole moments, are not

---

(8) The corresponding frequency in the ${}^3A_{2u}$ state of $Rh_2b_4{}^{2+}$ (b = 1,3-diisocyanopropane)[1] is 60 cm^{-1}. We favor a ligand-deformation assignment over various lattice-mode alternatives for both the 40- and 60-cm^{-1} vibrations because of structural similarities in the two binuclear bridging units.

(9) Spin–orbit coupling splits ${}^3A_{2u}$ into E_u and A_{1u} components. The $E_u({}^3A_{2u})$ state is expected to possess a significant transition moment because it can mix with the E_u state of ${}^1E_u(d\pi p\sigma)$ parentage. The transition to $A_{1u}({}^3A_{2u})$ is highly forbidden.

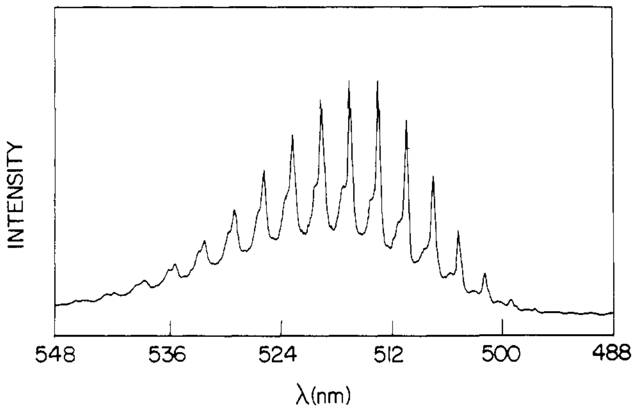

Figure 3. $^3A_{2u} \rightarrow {}^1A_{1g}$ (phosphorescence) spectrum of a single crystal of $K_4Pt_2(H_2P_2O_5)_4 \cdot 2H_2O$ at 10 K. λ_{ex} = 435 nm, instrumentation spectral resolution 1.6 Å.

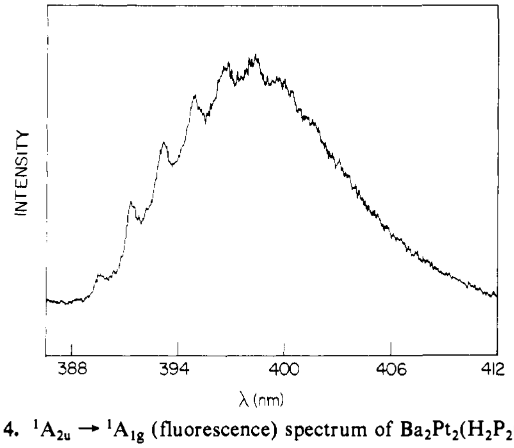

Figure 4. $^1A_{2u} \rightarrow {}^1A_{1g}$ (fluorescence) spectrum of $Ba_2Pt_2(H_2P_2O_5)_4$ at 10 K.

known in the barium salt. If the transition has vibronic-induced intensity, it is quite possible that its transition moments are not oriented along the same direction as the transition moments in $^3A_{2u}$. Furthermore, all the crystals examined may not have been oriented on the same face, resulting in variations in the ratio of intensities of this band to the $^1A_{1g} \rightarrow {}^3A_{2u}$. Whether this variation is explained by orientation discrepancies or perhaps low-symmetry defect-induced intensity, the excitation spectrum indicates that the ~400-nm band is attributable to $Pt_2(H_2P_2O_5)_4{}^{4-}$. The logical assignment for this band, because of the small distortion and very small change in the Pt–Pt vibrational frequency, is $^1A_{1g} \rightarrow {}^3A_{1g}$ ($d\sigma \rightarrow p\sigma$).

The single-crystal phosphorescence spectrum of $K_4Pt_2(H_2P_2O_5)_4 \cdot 2H_2O$ at 10 K is shown in Figure 3. The line widths in our vibrationally structured spectrum are much smaller than those reported previously,[7] and we suspect that impurities in the green microcrystalline material inhomogeneously broadened the lines.[10] Because we encountered so many problems in working with the potassium salt (see the supplementary material), we chose $Ba_2Pt_2(H_2P_2O_5)_4$ for further spectroscopic experiments.

The two emission bands of $Ba_2Pt_2(H_2P_2O_5)_4$ at 10 K are shown in Figures 4 and 5. The fluorescence forms a progression in a 110-cm^{-1} frequency (Figure 4), which is the ground-state Pt–Pt stretch, with the maximum occurring at least 6 quanta from the origin. An accurate measurement of the location of the origin was not made because the signal was very weak. The phosphorescence spectrum (Figure 5) is similar to that observed in the potassium salt. The spectrum is characterized by a progression in a 110-cm^{-1} vibration with a 40-cm^{-1} deformation mode built

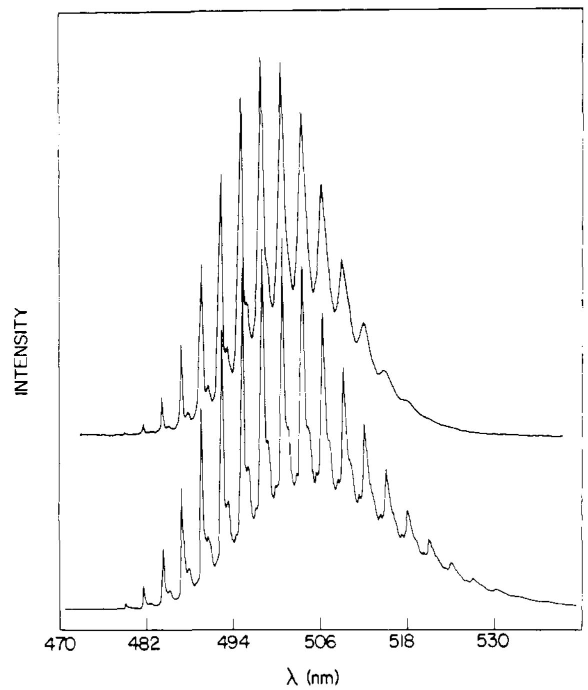

Figure 5. $^3A_{2u} \rightarrow {}^1A_{1g}$ (phosphorescence) spectrum of $Ba_2Pt_2(H_2P_2O_5)_4$ at 10 K (bottom); calculated spectrum (top).

on the principal lines. The Raman spectrum of $K_4Pt_2(H_2P_2O_5)_4$ has a band at 115 cm^{-1} that has been assigned to the Pt–Pt stretch in the ground state.[7] The 40-cm^{-1} mode is assumed to be the same ligand deformation as observed in the absorption spectrum. It may appear that there is a 40-cm^{-1} vibrational progression in this spectrum, because there are weak features at appropriate energies (80 and 120 cm^{-1}). However, the line at 80 cm^{-1} that is readily seen in the higher quanta of the Pt–Pt stretch is sharper than the 40-cm^{-1} vibration, suggesting that it is not the $v = 2$ level of a 40-cm^{-1} mode. In spite of the observation of this 60 or 40-cm^{-1} mode in three different spectra of $Rh_2b_4{}^{2+}$ [1] and $Pt_2(H_2P_2O_5)_4{}^{4-}$, its actual coordinate cannot be assigned with great certainty. The positions of all the lines observed in the phosphorescence spectrum of $Ba_2Pt_2(H_2P_2O_5)_4$ at 10 K are set out in Table II.

The highly structured emission and absorption bands in these samples of $Pt_2(H_2P_2O_5)_4{}^{4-}$ offered a rare opportunity to examine the applicability of a Franck–Condon analysis. Neither the ground- nor the excited-state vibrational frequencies were allowed to vary in the calculation; thus the only adjustable parameter that determined the overall shape of the band was $\Delta\zeta$, the mass-normalized displacement of the upper and lower potential surfaces. The results are shown in Figures 5 and 6. The best fits for the emission and absorption bands were calculated by standard procedures from overlaps of the vibrational wave functions of two displaced quadratic potential surfaces.[11,12]

The calculated displacements[13] for emission (0.24 Å) and absorption (0.19 Å) are nearly the same (and are within acceptable error limits).[14] These values yield an average displacement of 0.21 Å.[15] This distortion is considered to be a contraction in the

---

(10) It is likely that surface (or defect) ions inhomogeneously broaden the lines in microcrystalline samples (Hochstrasser, R. M.; Brasad, P. N. "Excited States" Lim E. C., Ed.; Academic Press: New York, 1974; Vol. 1, p 103). Indeed, we have found that pure yellow samples of $K_4Pt_2(H_2P_2O_5)_4$ exhibit broader spectral lines when crushed (powdered).

(11) Ballhausen, C. J. "Molecular Electronic Structures of Transition Metal Complexes"; McGraw-Hill: London, 1979; pp 132–135.

(12) Parameters necessary for calculations such as line widths and the intensity of the 40-cm^{-1} deformation mode were taken directly from the spectra. The line shapes of the individual lines were assumed to be Lorentzian. A Gaussian line shape did not adequately provide for the intensity seen in the spectrum between the sharp peaks. The Lorentzian shape indicates that the broadening is homogeneous and does not depend on site defect distribution (Rice, S. F. Ph.D. Thesis, California Institute of Technology, 1982).

(13) In the calculation it was assumed that the metal–metal stretch is simply that of two platinum atoms. Inclusion of other effective masses such as for the four ligating phosphorus atoms will serve to decrease the size of this distortion.

(14) Because of the change in line width of the dominant lines in the spectrum as a function of metal–metal quantum number, the accuracy of this calculation is limited to errors on the order of 10–15% in the net distortion.

Table II. Positions and Spacings between the Lines in the $^3A_{2u} \rightarrow {}^1A_{1g}$ Phosphorescence Spectrum of $Ba_2Pt_2(H_2P_2O_5)_4$ at 10 K

V[a]	E_v, cm^{-1}	Δ[b]	$E_v - E_{v-1}$
0	20987		
	20947	40	
1	20877		110
	20835	42	
2	20766		111
	20724	42	
3	20654		112
	20613	41	
4	20542		112
	20500	42	
	20456		
5	20427		115
	20385	42	
	20342		
6	20312		115
	20271	41	
	20228		
7	20198		114
	20158	40	
	20115		
8	20088		110
	20051	37	
	20006		
9	19978		110
	19940	38	
	19896		
10	19868		110
	19831	37	
	19786		
11	19758		110
	19716	42	
	19672		
12	19644		114
	19603	41	
	19561		
13	19530		114
	19516		
	19489	41	
14	19447		
	19417		113
	19404		
	19375	42	
	19336		
15	19308		109
	19291		
	19266	42	
	19226		
16	19198		110
	19183		
	19157	41	
	19117		
17	19088		110
	19007		
18	19978		110
19	18864		114
20	18751		113
21	18639		112

[a] The assigned a_{1g}(Pt–Pt) vibrational quantum number.
[b] Spacings between the principal peaks in the progression and the secondary (ligand deformation) peaks.

Pt–Pt distance because the ground-state frequency is much lower than that of the excited state, as is the case for $Rh_2b_4^{2+}$.

Both the ground-state (2.92 Å) and the calculated $^3A_{2u}$ (2.71 Å) Pt–Pt distances in $Pt_2(H_2P_2O_5)_4^{4-}$ are significantly shorter than the corresponding Rh–Rh distances in $Rh_2b_4^{2+}$ (3.24 Å, ground state; 2.90 Å, $^3A_{2u}$).[1] The estimated force constants for M–M stretching (diatomic approximation) show clearly that the Pt–Pt

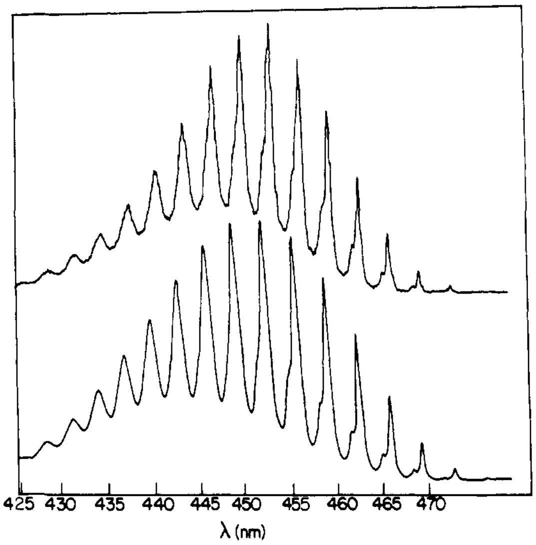

Figure 6. Comparison of the experimental (top) $^1A_{1g} \rightarrow {}^3A_{2u}$ absorption spectrum of $Ba_2Pt_2(H_2P_2O_5)_4$ with the calculated spectrum.

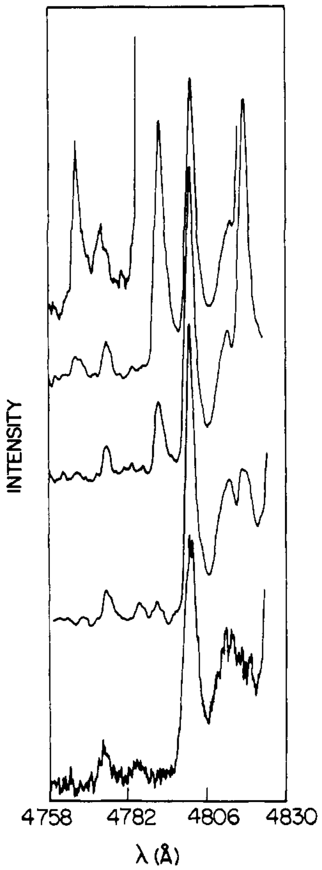

Figure 7. Temperature dependence of the $^3A_{2u} \rightarrow {}^1A_{1g}$ origin region in the spectrum of $Ba_2Pt_2(H_2P_2O_5)_4$. Top to bottom: 8, 7.5, 6.4, 5.2, 4.2 K.

bond (0.69 mdyn/Å) is much tighter than Rh–Rh (0.21 mdyn/Å) in the ground states of these $d^8 \cdot d^8$ coupled systems. We would have expected that the dσ bonding would follow the order 4d < 5d, but the extent of the difference suggests that the relatively constraining P–O–P bridging unit plays a significant role in the larger Pt–Pt interaction.

The temperature dependence of the origin region of the $Ba_2Pt_2(H_2P_2O_5)_4$ phosphorescence is shown in Figure 7. The origin obviously loses intensity rapidly as the temperature is lowered. A band appears at 477.48 nm, 40.9 cm^{-1} below the 476.55-nm origin. The energies of all the lines observed in the 4.2 K spectrum (Figure 8) of $Ba_2Pt_2(H_2P_2O_5)_4$ are given in Table III. Most of

---

(15) This value differs from the 0.438 Å reported in ref 7; the discrepancy is due mainly to omission of π in the expression $\Delta r = b(2\pi M\omega_0/h)^{-1/2}$. Inclusion of $(\pi)^{-1/2}$ in the earlier analysis[7] gives Δr = 0.247 Å, which is in excellent agreement with the value (0.24 Å) we have estimated from emission data.

Table III. Positions and Spacings between the Lines in the $^3A_{2u} \rightarrow {}^1A_{1g}$ Phosphorescence Spectrum of $Ba_2Pt_2(H_2P_2O_5)_4$ at 4.2 K

V^a	E_v, cm^{-1}	Δ^b	$E_v - E_{v-1}$
0	20943		
	20899	44	
1	20828		115
	20781	47	
2	20722		106
	20672	50	
3	20610		112
	20560	50	
	20536		
4	20496		114
	20445	51	
	20429		
5	20383		113
	20329	54	
	20311		
6	20269		114
	20220	49	
	20200		
7	20157		112
	20106	51	
	20088		
8	20045		112
	20000	45	
	19978		
9	19934		111
	19890	44	
	19866		
10	19825		109
	19780	45	
	19757		
11	19713		112
	19667	46	
	19641		
12	19600		113
	19554	46	
	19529		
13	19489		111
	19440	49	
	19412		
14	19372		117
	19330	42	
	19305		
	19194		
	19084		
	18975		
	18868		

[a] The assigned a_{1g}(Pt-Pt) vibrational quantum number.
[b] Spacings between the principal peaks in the progression and the secondary (ligand deformation) peaks.

the lines (10 or 4.2 K) are readily interpretable in terms of either the 476.55- or the 477.48-nm origin. In each case a broadened 40-cm^{-1} vibration is built on a 110-cm^{-1} progression.

The results reported here show conclusively that $Ba_2Pt_2(H_2P_2O_5)_4$ possesses two emitting states that are split by 40.9 cm^{-1}. According to Fordyce, Brummer, and Crosby,[7] these states should be assigned to the E_u and A_{1u} components of $^3A_{2u}$, with A_{1u} at lower energy.[16] One slight problem with this assignment scheme is that the bands that appear to be built on the E_u origin have a puzzling intensity distribution at 4.2 K. As the Pt-Pt quantum number increases, these lines begin to dominate the intensity of the system and appear to become more intense than the bands built on the A_{1u} origin. In addition, the apparent maximum of this overall emission system occurs at $v = 11$ (several quanta different from the maximum at 10 K), thereby indicating that the A_{1u} triplet component distorts differently than the E_u. Although it should be recognized that other assignments for the two emitting components cannot be ruled out entirely,[17] the reasonable conclusion at this point is that zero-field-split E_u and A_{1u} components of $^3A_{2u}$ account satisfactorily for the bulk of the experimental information available.

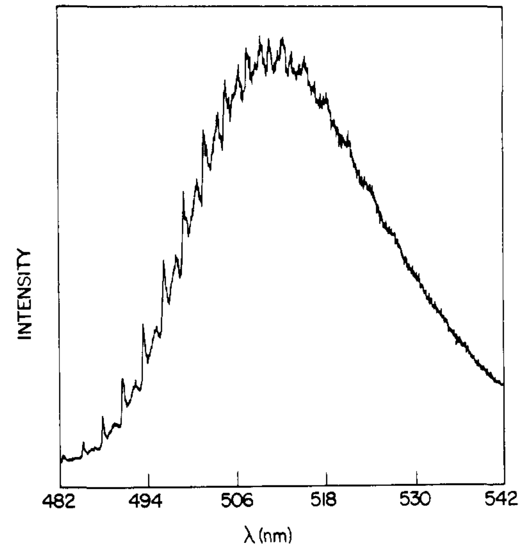

Figure 8. $^3A_{2u} \rightarrow {}^1A_{1g}$ (phosphorescence) spectrum of $Ba_2Pt_2(H_2P_2O_5)_4$ at 4.2 K.

Acknowledgment. We thank V. M. Miskowski and R. E. Marsh for helpful discussions. S.F.R is grateful to the Fannie and John Hertz Foundation for financial support. This research was supported by National Science Foundation Grants CHE78-10530 and CHE81-20419.

Registry No. $Pt_2(H_2P_2O_5)_4^{4-}$, 85565-26-0; $Ba_2Pt_2(H_2Pt_2O_5)_4$, 85565-27-1.

Supplementary Material Available: Properties and absorption spectra of various samples of $K_4Pt_2(H_2P_2O_5)_4 \cdot 2H_2O$ (4 pages). Ordering information is given on any current masthead page.

---

(16) The phosphorescence lifetime of $K_4Pt_2(H_2P_2O_5)_4 \cdot 2H_2O$ is 640 μs at 9 K and 10.3 μs at 77 K.[7] As the temperature is lowered to 4.2 K, there is no longer an appreciable population in the higher E_u state to overwhelm the A_{1u} emission. The lifetime is then observed to be much longer than that of the E_u state, which has a much larger oscillator strength.[9]

(17) An alternative model that is consistent with our experiments involves a double-welled potential along a coordinate other than Pt-Pt for the excited triplet. Another possibility is that the excited-state splitting is attributable to solid-state effects. The suspicious coincidence of additional lines about 40 cm^{-1} away from the origin in both absorption and emission is a source of concern in connection with the favored interpretation.